Journal of Thermal Analysis and Calorimetry
https://doi.org/10.1007/s10973-024-13059-x

Thermodynamic analysis of drying cycles utilizing a desiccant wheel thermoelectric modules and heat pipe for the drying of hazel nuts in the East Blacksea climatic conditions

Betül Saraç[1,2,3] · Cevdet Demirtaş[1,2,3] · Teoman Ayhan[1,2,3]

Received: 27 July 2023 / Accepted: 8 March 2024
© The Author(s) 2024

Abstract

The use of renewable energy sources to maintain appropriate thermal humidity and temperature conditions in food drying technologies, especially in humid climate zones, is a current area of research. In the Eastern Black Sea Region, the high relative and specific humidity of the atmospheric air lead to a low drying rate of the products. Therefore, in this study, to enhance the drying rate of the products, three models and their psychometric cycles were studied on decreasing the specific humidity of the drying air and increasing the moisture saturation degree of the drying air. The innovative hazelnut drying models proposed for the climatic conditions of the Eastern Black Sea region incorporate several components, including thermoelectric modules (TEM), photovoltaic thermal (PV/T) systems, desiccant wheels (DW), heat pipes (HP) and heat exchangers (HX). The thermodynamic analysis was conducted on the theoretical cycles belonging proposed models. Emphasis was given to the development of Model-C, taking into account the drying conditions specific to hazelnuts in the Eastern Black Sea region, among the cycles named Model-A, Model-B and Model-C. The energy efficiencies and SEMER values of Model-A, Model-B and Model-C were presented based on selected atmospheric conditions. Each model is valid under its characteristic operating conditions, and the energy efficiencies, SEMER values and the exergetic efficiencies for Model-A, Model-B and Model-C were determined as (4.66%-0.271 kg-H_2O kWh^{-1}–62%), (9.87%-0.1542 kg-H_2O kWh^{-1}–22%) and (9.13%-0.1381 kg-H_2O kWh^{-1}–10%), respectively. Also, presented models of hazelnut drying supported by renewable energy have achieved high sustainable index (SI) values. Consequently, these models ensure the sustainability of energy in the drying sector and facilitate the assessment of their environmental, economic and social impacts. The utilization of renewable energy in the models will lead to a reduction in CO_2 emissions during the drying process. These results indicate that TEM systems are a viable option for food drying in the future.

Keywords Photovoltaic thermal · Thermoelectric modules · Desiccant wheel · Drying · Hazelnuts · Energy · Exergy

Abbreviations

db	Dry bulb
wp	Wet product
o	Dead state condition
a	Air
v	Vapour
d	Destruction
L	Loss

List of symbols

T	Temperature (°C)
P	Pressure (Pa)
h	Enthalpy (kJ kg^{-1})
Ex	Exergy (kJ kg^{-1})
w, *x*	Specific humidity of air (kg $H_2O.kg^{-1}$ dry air)
RH	Relative humidity of air (%)
M	Mass (kg)
C	Specific heat (kJ kg^{-1} K^{-1})
R	Gas constant of air (kJ kg^{-1} K^{-1})
$\dot{W}$	Power (kW)
$\dot{Q}$	Heat rate (kW)

✉ Betül Saraç
bsarac@ktu.edu.tr

[1] Department of Naval Architecture and Marine Engineering, Karadeniz Technical University, Sürmene, Trabzon, Turkey

[2] Mechanical Engineering Department, Karadeniz Technical University, Trabzon, Turkey

[3] 18/12, Soğanlı Sokak, 61080 Trabzon, Turkey

Published online: 09 April 2024

Introductions

In recent years, studies on integrating TEM into moisture-absorbing refrigerated air conditioning systems to investigate their effects on the cooling performance of air conditioning systems have gained attention among researchers. In thermoelectric cooling, there are no refrigerant fluids, piping circuits or compressors. The investigation of various applications and performance efficiencies of air heating and cooling cycles integrated with TEM has drawn significant attention. Despite the relatively lower energy efficiency of motionless (TEM) systems compared to heat pump systems, the proximity of SEMER values to those achieved in food drying with heat pump systems suggests the potential applicability of TEMs in this domain. SEMER values for vapour compression heat pump systems typically range from 0.26 to 0.50, depending on atmospheric climate conditions, the specific product being dried and the system type. In this study, the obtained SEMER value was found to be close to the values reported in the literature for heat pump studies. Thermal comfort and air quality have gained importance in climate control systems with thermoelectric module technology, as they increase energy efficiency and reduce greenhouse gas emissions. Research on various food drying technologies using renewable energy sources is ongoing in the literature.

Ceylan and Ergun [1] conducted a psychometric analysis on drying pine and poplar wood in a heat pump dryer to investigate the relationship between humid air and thermodynamics. The mass change in the drying unit was analysed with energy. Pandey et al. [2] designed as a natural and forced mode solar cabinet dryer with a loading capacity of 2 kg of fresh product, and it is stated that drying the pepper in natural mode is 50–56 h, and drying in forced mode takes approximately 10 h depending on whether the heater is used as an external heat source or not. Ye et al. [3] presented more effective and ecologically friendly drying methods in terms of energy consumption by studying the energy consumption and specific energy requirements of mint leaves in various drying processes. Akbulut and Durmuş [4] used a forced solar drier to perform thin-layer drying tests on mulberry and examined the impact of inlet air velocity and drying duration on energy and exergy at five different drying mass flow rates. They concluded that when drying mass flow rate increased, energy utilization ratio and energy loss reduced while exergetic efficiency improved. Caliskan et al. [5] evaluated the performance of a newly developed desiccant air ventilation system consisting of a desiccant wheel, sensible heat wheel and evaporative air cooler. They conducted energy, exergy and sustainability analyses to compare the system's performance with previous studies.

Saraç [6] aimed to evaluate the utilization of waste heat from tea factories in cooling systems in the Eastern Black Sea region. The study presented three different types of air conditioning systems that could be used for climate control in indoor and living spaces during the summer months. It was emphasized that utilizing the waste air discharged from tea factories as direct regeneration air greatly contributed to bringing the outdoor air humidity to comfort conditions. By determining the lower and upper limits of thermodynamic usability, the study focused on how to utilize this waste heat most efficiently. In the study conducted by [7], the thermodynamic feasibility of utilizing waste heat from a ship and applying it to a desiccant-evaporative cooling system for air conditioning purposes was examined. Three different air conditioning models were presented, and their thermodynamic potential for utilization was assessed. The second air conditioning model was identified as the most promising cycle for air conditioning applications in hot and humid climate regions. Saraç et al. [8] applied exergy and advanced exergy analysis to a model comprising an air conditioning unit consisting of an air mixture connection, evaporator, heater and fan to cool a living space under summer conditions. They demonstrated the applicability of exergy analysis and advanced exergy analysis methods to air conditioning systems. Gungor et al. [9] investigated the efficiency of a pilot-scale gas engine-driven heat pump dryer by drying three medicinal and aromatic plants using exergy analysis. The drying experiments were conducted at an air temperature of 45 °C. In this study, the performance of the dryer and its main components were evaluated using the exergy analysis method. They reported that the gas engine was the most important component for improving the system efficiency, while the exhaust air heat exchanger played a crucial role in the drying system. Giannetti et al. [10] combined experimental and theoretical approaches to evaluate the performance of different desiccant systems, obtaining valuable insights into their efficiency and sustainability. They obtained findings that could contribute to the design of more efficient drying systems in the future. Rafique et al. [11] have conducted a study to investigate the performance of a solar desiccant cooling system by developing a theoretical model and conducting energy and exergy analyses.

In the study conducted by [12], a solid desiccant-assisted hybrid air conditioning system was designed, and its performance was determined through thermodynamic analysis. Based on experimental results, it was reported that this system could be a suitable solution for providing thermal comfort to individuals in hot and humid climates while utilizing low electrical energy. Patel and Kar [13] conducted a review study presenting the recent advancements in heat pump drying, which encompassed the working principle, efficiency and applications of heat pump drying for drying agricultural products. Sharma et al. [14] performed an exergy analysis

to evaluate the performance of single-stage and multistage thermoelectric coolers. They compared the performance of these coolers using parameters such as cooling rate, coefficient of performance, second law efficiency and exergy destruction. Kara et al. [15] performed an exergy analysis of a designed adsorption-based desiccant air conditioning system to evaluate its usability under Yozgat climate conditions and the potential for enhancing its performance by utilizing waste heat or renewable energy sources for regeneration heat. According to [16], they found that the mixed drying system, which involved the addition of an auxiliary heater to the solar drying system, achieved higher efficiency compared to the solar drying system. Kuzgunkaya and Hepbasli [17] conducted an exergy analysis of a designed heat pump drying system for laurel leaves. They stated that the exergy efficiency of the dryer increases as the drying air temperature increases. Akpinar [18] conducted a study on the thin-layer drying characteristics of mint leaves in a forced convection solar dryer and under natural convection of open sun and performed energy and exergy analyses for the drying process. The drying data were fitted to ten different mathematical models, and among them, the Wang and Singh model for forced solar drying and natural sun drying was found to best explain the thin-layer drying behaviour of mint leaves. Through energy and exergy analysis, [19] assessed the impact of various weather conditions on the effectiveness of drying mint leaves and the thermodynamic performance of the process using an air source heat pump drier. In the study, experimental research was done to determine the effect of various weather conditions on the effectiveness of drying mint leaves. The study's results, according to the authors, would help drying systems operate more effectively. Gómez-de la Cruz et al. [20] performed an energy and exergy analysis on the rotary dryer used to dry olive pomace. In their experimental study using various dryer air temperatures and air velocities, they found that the high moisture content and high temperature of the by-product combined with the drying air flow resulted in a significant thermal shock in the first third of the trommel, which caused the moisture content of the olive pomace to be reduced by half. The characteristics that impact the performance of the plant were determined by [21] through parametric research based on energy and exergy analysis of a rotary dryer used for drying the ingredients in the aggregate mixture of a hot mix asphalt plant. Luo et al. [22] simulated the system to evaluate the exergetic and economic performance of a transcritical heat pump refrigeration system employing CO_2 as the working fluid in hot regions. Dincer and Sahin [23] have developed a new exergy-based model for thermodynamic analysis and presented an example study to demonstrate its applicability to a real drying process. They emphasized that their proposed model would be useful for researchers in designing drying systems, optimizing their components and determining the most suitable configurations. Bardant et al. [24] carried out a study, examined various environmental indicators, including the renewability and level of perfection of Gamboeng tea, assessed the energy efficiency of the tea factory using an exergy analysis and offered suggestions on how Gamboeng tea can be made more sustainable and energy efficient. Energy and exergy studies of a commercial wood chip drying process were carried out in the study by [25], and recommendations were given to increase the operation's energy and exergy effectiveness. Hossain et al. [26] evaluated the performance of a cabinet solar dryer experimentally to assess the drying characteristics, energy and exergy efficiency and drying speed of red pepper in Bangladesh.

In hazelnut drying processes, the use of TEM for conditioning the drying air has become important in terms of increasing energy efficiency and reducing greenhouse gas emissions. Demirtaş [27] reported that removing the moisture from the air and allowing hazelnuts to dry can positively impact the aroma of hazelnuts and in addition conducted research on the effect of 0.45, 0.55, 0.60 and 0.70 relative humidity values of drying air on drying time. He stated that the drying time increased at high relative humidity values, and as a result, the moisture content of hazelnuts was higher after drying. This high moisture content, he noted, can cause the aroma to deteriorate rapidly. It is known that the drying of individual fruits is influenced by the first-degree drying air temperature, the second-degree relative humidity of the air and the third-degree velocity of the air, [28]. Due to the climatic conditions in the regions where hazelnuts are grown in Turkey, the drying process is attempted to be carried out under atmospheric relative humidity conditions. This proves to be quite laborious for the producers and increases both the drying time and costs. Interesting research areas have emerged where solar energy systems technologies and TEM systems are combined. The thermodynamic analysis of combined systems integrating solar energy systems Technologic developments and TEM systems has gained attention in the literature. In this regard, different thermodynamic cycles for the applications of solar energy drying, TEM, desiccant wheel (DW) and heat pipe (HP) in the hazelnut drying process in the Black Sea region have been discussed in this study.

The novelty of the study lies in the thermodynamic analysis of drying cycles that incorporate a DW, heat exchangers (HX), PV/T and HP into the system to address the inconsistencies in the cabin energy balance caused by the use of TEM in drying processes reliant on solar energy for hazelnuts. These drying cycles aim to maintain a constant drying air temperature of 43 °C during the air conditioning processes conducted with TEM.

In the literature, in order to preserve the aroma of hazelnuts during the drying process, it is required that the

drying air temperature does not exceed 43 °C. Introducing the air conditioning unit operated by TEM into the literature to meet this requirement and to maintain the specific humidity of the drying air at low levels is the innovative aspect of this study. For this purpose, a thermodynamic analysis of drying cycles integrating a DW, heat exchangers (HX), PV/T and HP into the system has been conducted to address the inconsistencies in the cabin energy balance arising from the use of TEM in solar energy-based drying processes for hazelnuts.

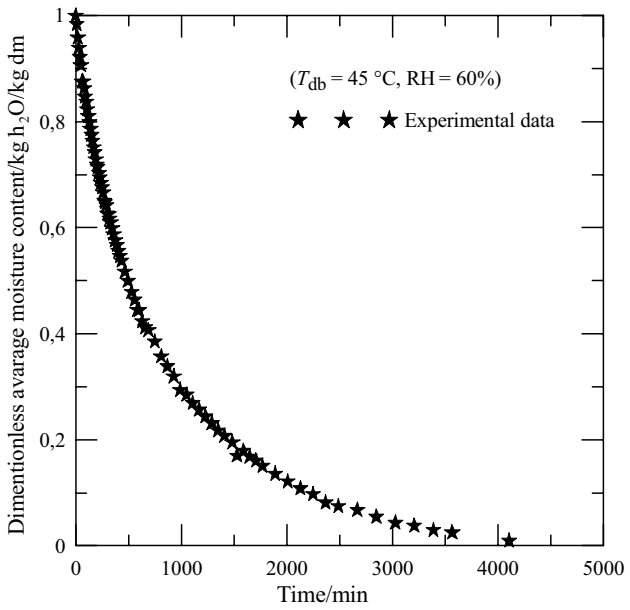


Fig. 1 The dimensionless average moisture content of hazelnuts versus time (minutes) [27]

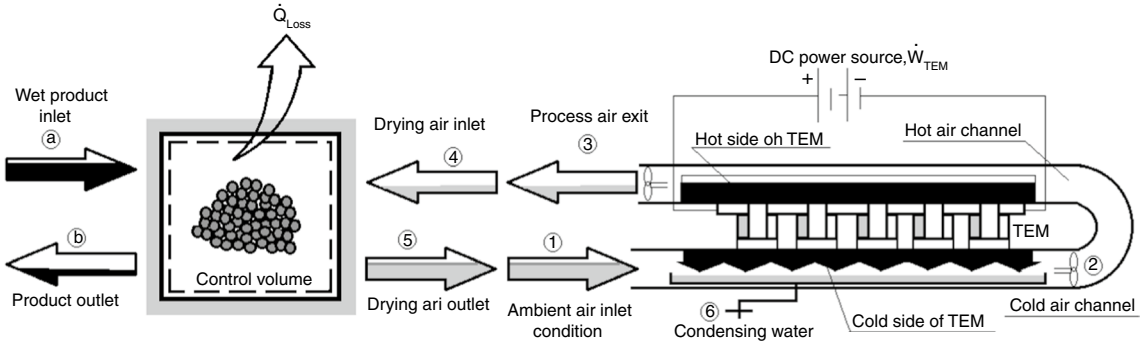
Materials and methods

Material

The experimental data for the hazelnut drying performance used in the study were obtained from the doctoral thesis [27]. Demirtaş [27] has been determined that the hazelnut drying process takes 4100 min to complete. According to [28], it is stated that the drying time of hazelnuts is completed in approximately 3 days. This study was conducted based on these data (Fig. 1).

System description

Figure 2 presents the schematic of a drying cabinet and a novel TEM air conditioning unit as the two main units of hazelnut drying systems. These two units and other energy transport systems are combined in the open cycles considered. The drying cabinet is dimensioned according to 100 kg (based on wet mass) hazelnut capacity, and its dimensions are calculated to be 0.6 m*0.60 m*1.0 m according to the thin-layer drying model. Since the drying air temperature in the hazelnut drying processes is recommended as 40 °C in the literature, the cabin ambient air temperature was kept constant at 40 °C in this study. The total heat transfer coefficient was valid on the walls, base and ceiling of the drying cabinet and was selected as U = 0.86 Wm^{-2} °C. An outlet vent was considered towards the upper end of the cabinet to facilitate and control the convection flow of air through the dryer (Point 5 shown in Fig. 2a). The new TEM air conditioner consists of four components: TEM, heat sink (HS), cold storage mass (HCM) and fans (Fig. 2b). In the new TEM air conditioner, the reduction of atmospheric air absolute humidity below the absolute humidity at the air dew point temperature and then heating and raising the process



(a) Drying cabinet (b) TEM-operated air conditioning system

Fig. 2 The model of the drying cabinet and TEM system

air temperature to 43 °C is calculated by the flow conditions in the cold air duct and hot air duct. The air mass flow rate is adjusted so that the supply air temperature exiting the hot air duct is 5 degrees lower than the operating temperature of the TEM unit modules, to protect Peltier modules. Instead of wasting the excess heat generated here into the environment, the recovery of waste heat is ensured. Separate cycles were designed for each climatic zone and examined by naming them Model-A, Model-B and Model-C.

In the drying system incorporating a new TEM unit, which operates in conjunction with a DW, PV/T, heat exchangers and a heat pipe, three different cycles have been thermodynamically analysed to minimize the required energy for the drying cabinet and adapt to climatic zones, (climatic zone-A, climatic zone-B and climatic zone-C) conditions. The dry bulb temperature and relative humidity of the atmospheric air were obtained from meteorological statistical data as follows: in climatic zone-A, 38 °C and 85%; in climatic zone-B, 30 °C and 75%; and in climatic zone-C, 23.5 °C and 70% are shown in individual figures. In the Eastern Black Sea region, hazelnut harvesting and drying season occurs in July and August. According to meteorological statistical data, the atmospheric conditions in climatic zone-C align with the hazelnut harvesting and drying season during July and August. Therefore, in the presented study, the performance of the proposed Model-C is considered for hazelnut drying processes.

Psychometric cycle modelling and basic principles

The following assumptions were made for the cycles modelling and analysis in this work:

1. The bypass factor (BF) in the cold and hot air flow channels is assumed to be 0.13.
2. The effectiveness of the heat source and cold storage block is 85%.
3. The quantity of fresh hazelnuts in the drying chamber is assumed to be 100 kg.
4. The drying process time was selected for three days concerning literature data.
5. The thermal and electrical contact resistances in the structure of the heat source and cold storage block are not considered. The operating temperature of the Peltier devices was maintained at 55 °C.
6. The modelling of all cycles is completed under steady-state conditions.
7. The drying cabinet air temperature is maintained at 40 °C, and the supply air temperature is also kept at 43 °C throughout the entire process. The pressure drops in duct lines, hot and cold air channels, heat exchangers, as well as within the mixer and the splitter are neglected.
8. The moisture drop of the hazelnuts was modelled 35% to 6% as requested by hazelnut producers.
9. The supply air conditions at the entrance of the drying cabinet were selected as the recommended temperature in the literature 43 °C.
10. The reference values for efficiency factors used to evaluate the performance of a desiccant wheel are typically chosen to achieve high levels of mass transfer effectiveness, which is around 0.9, and enthalpy effectiveness, which is approximately 0.1 [29].
11. The efficiency of a heat pipe is typically selected as 50% when the evaporation temperature is 55 °C.
12. In the modelling of TEM units, assuming a temperature difference of approximately 45 °C within the TEM unit and an average atmospheric air temperature of 30 °C, based on the database in reference [30], the coefficient of performance $\left(COP_{\mathrm{RF}}\right)$ on the cooling side has been selected as 1/3. Using the energy balance equation, $COP_{\mathrm{HP}} = 2/3$ was calculated.
13. The efficiencies of heat exchangers are taken between 75 and 85%.

Methodology

Range of conditions studied in the parametric study:

a. Outdoor temperature: (23.5 °C ~ 38 °C)
b. Outdoor relative humidity: (75% RH ~ 85%RH)

Three climatic zones in this range are shown in the psychometric chart:

a. Climatic zone-A (38 °C and 85% RH), apparatus dew point temperature 24 °C
b. Climatic zone-B (30 °C and 75% RH), apparatus dew point temperature 19 °C
c. Climatic zone-C (23.5 °C and 70%RH), apparatus dew point temperature 12 °C

The apparatus dew point temperatures were selected based on the operating conditions of the TEM components and the limits of the atmospheric air dew point temperature.

Model descriptions and the cycles

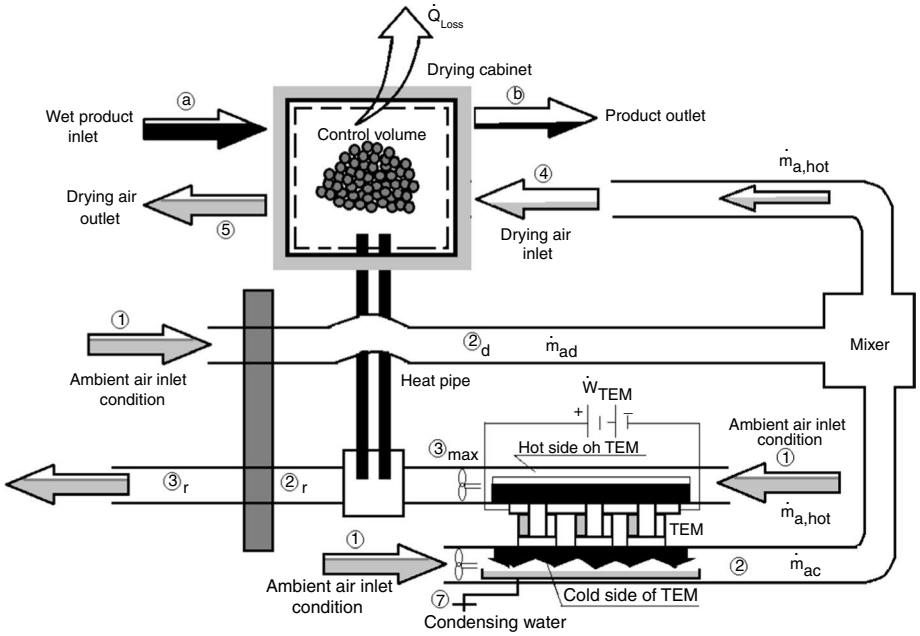
In this study, the climatic conditions where Model-A, Model-B and Model-C systems are applied (climatic zone-A, climatic zone-B and climatic zone-C) have been considered. The operational conditions of the models, including psychrometric cycles and thermodynamic analyses, have been examined as well.

Model-A

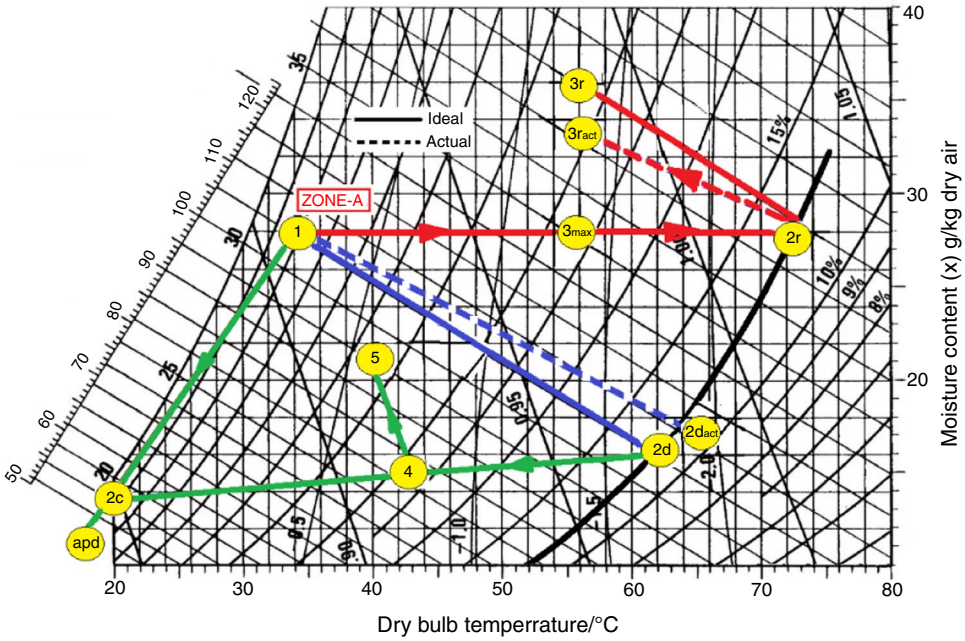
Model-A consists of a drying chamber, an air mixing chamber, a heat pipe and a TEM. The model-A drying cycle is designed based on climatic zone-A values. The schematic diagram of the drying system is shown in Fig. 3a, and the points of the cycle on the psychometric chart are given in Fig. 3b.

Model-B

Model-B consists of a drying chamber, an air mixing chamber, an HP, one heat exchanger (HX2) and one air heating duct (HX1) and one TEM. The energy supply for the air heating duct can be achieved employing a photovoltaic thermal system PV/T. Model-B drying cycle is designed based on climatic zone-B values. The schematic diagram of the



(a) Layout of the Model-A



(b) The psychometric cycle of the Model-A

Fig. 3 **a** Layout of the Model-A. **b** The psychometric cycle of the Model-A

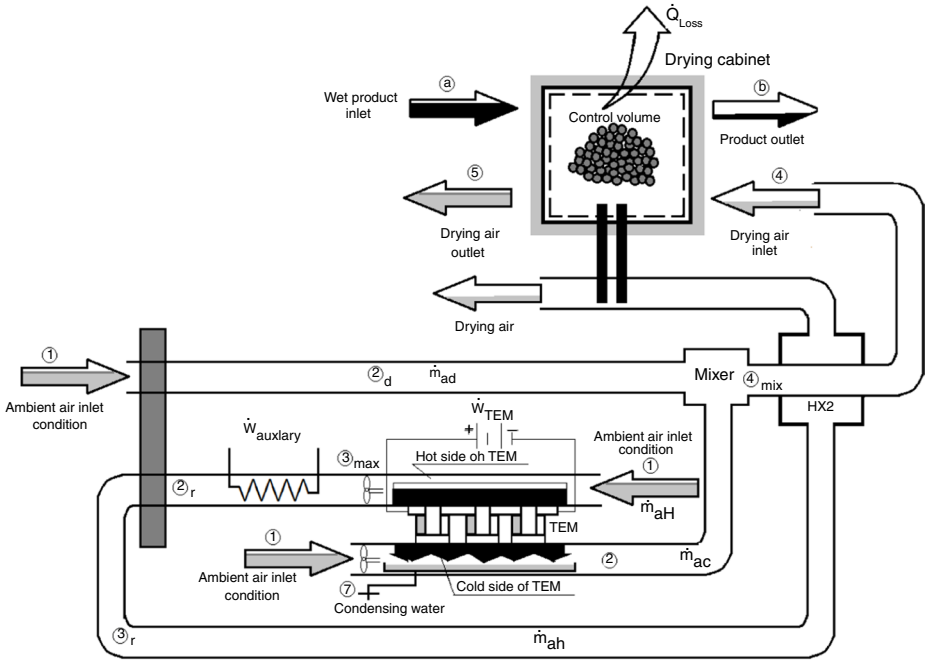
drying system is shown in Fig. 4a, and the points of the cycle on the psychometric chart are given in Fig. 4b.

Model-C

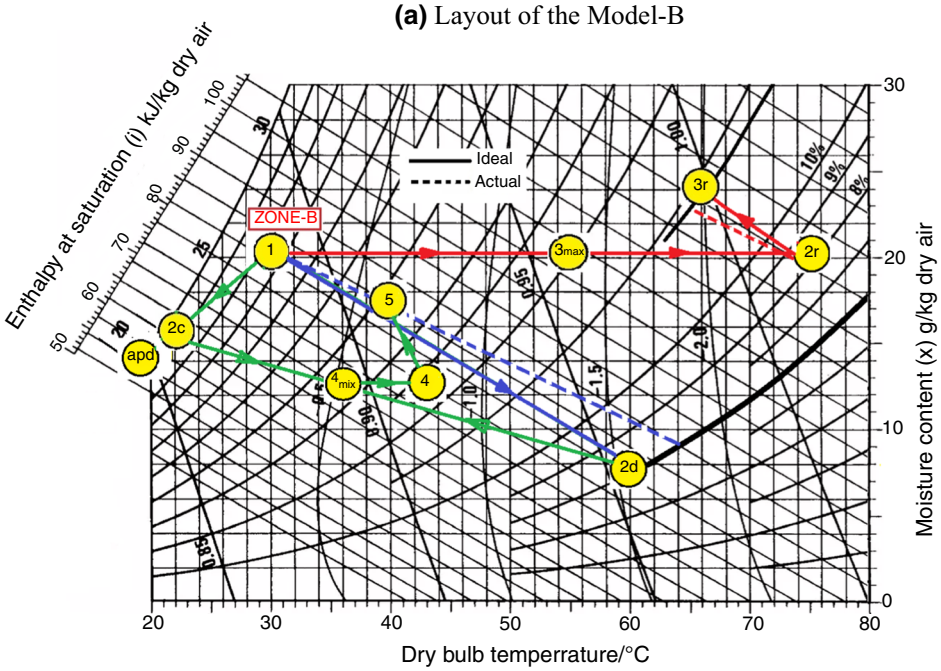
Model-C consists of a drying chamber, an air mixing chamber, an HP, one heat exchanger (HX2) and two air heating ducts (HX1) and one TEM. The energy supply for the air heating ducts can be achieved by means of a PV/T system. Model-C drying cycle is designed based on climatic zone-C values. The schematic diagram of the drying system is shown in Fig. 5a, and the points of the cycle on the psychometric chart are given in Fig. 5b.

Drying cabinet conditions

Equation 1 was used to determine the quantity of moisture removed from a $M_{product}$100 kg wet product. The drying

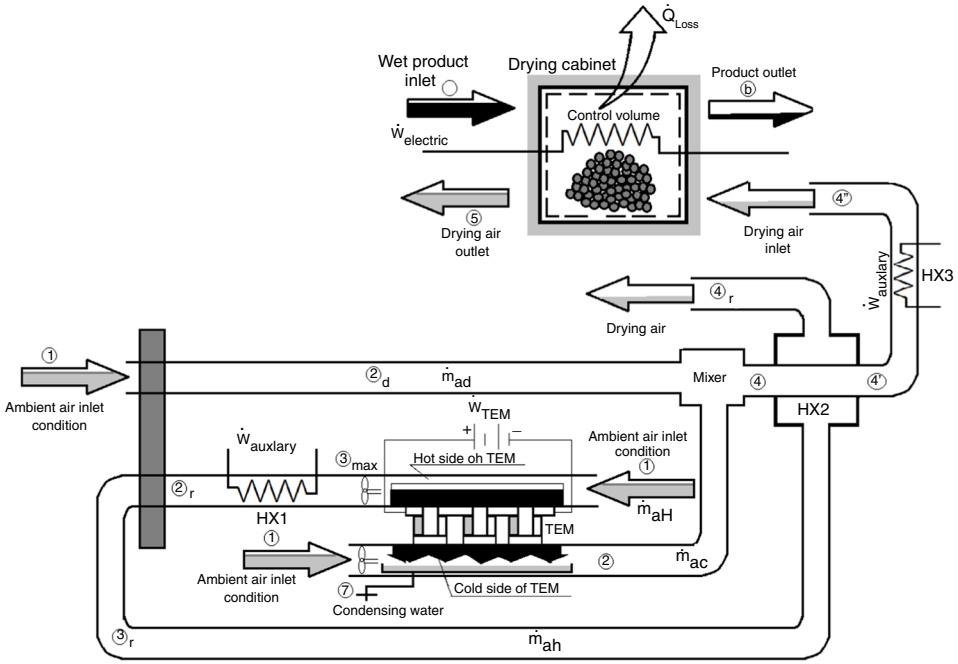


(a) Layout of the Model-B

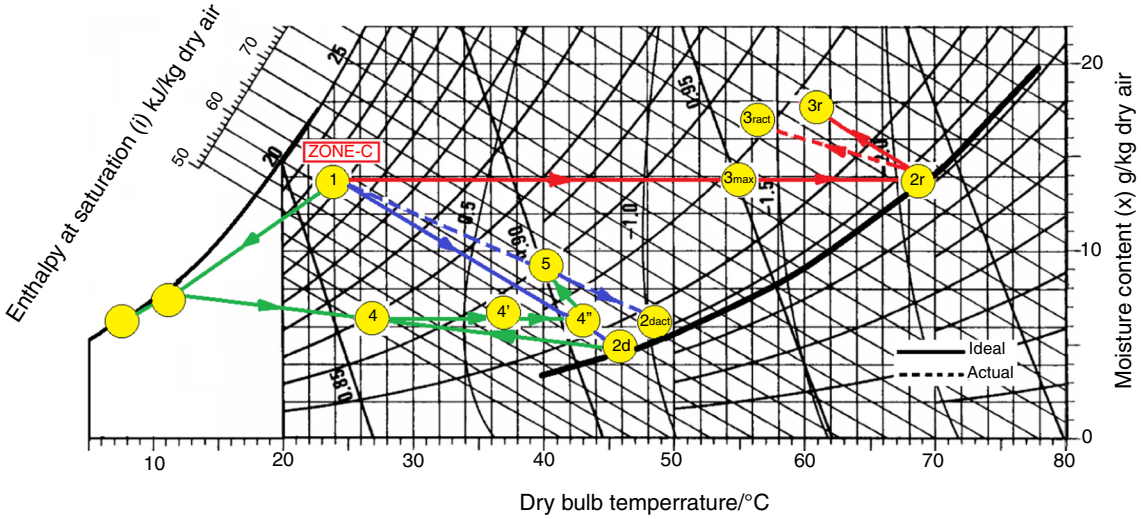


(b) The psychometric cycle of the Model-B

Fig. 4 **a** Layout of the Model-B. **b** The psychometric cycle of the Model-B



(a) The layout of the Model-C



(b) The psychometric cycle of the Model-C

Fig. 5 **a** The layout of the Model-C. **b** The psychometric cycle of the Model-C

air temperature in the cabinet was set at $T_{\text{cabinet}} = 40$ °C, and the drying duration was assumed to be $\Delta t = 3$ days, equivalent to 72 h [28].

$$M_{\text{moisture}} = \frac{M_{\text{wp}}\left(X_1 - X_2\right)}{\left(1 - X_2\right)}\left[\text{kg_H}_2\text{O}\right] \tag{1}$$

The product drying rate ($\dot{m}_{\text{wp}}$) was defined as the relationship between the initial moisture content of the wet product and the drying time (seconds) during the shift from the initial moisture content to the final moisture content value (Fig. 6).

$$\dot{m}_{\text{wp}} = \frac{M_{\text{wp}}}{\Delta t}\left[\frac{\text{kg_product}}{s}\right] \tag{2}$$

A commonly used performance parameter for the drying system is the specific moisture extraction rate (SMER), which is defined as follows [31].

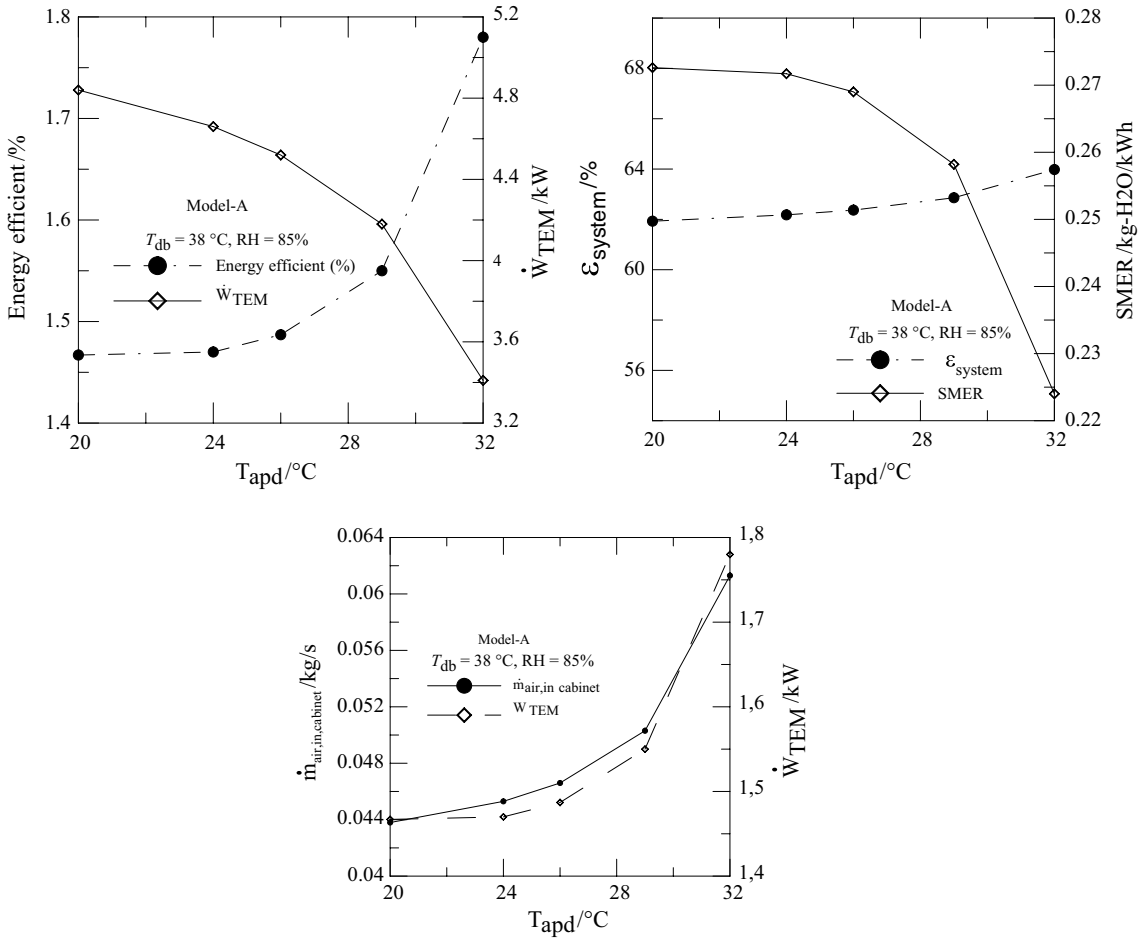


Fig. 6 The variation of performance parameters of Model-A with respect to T_{apd} temperature

$$\text{SMER} = \frac{\text{amount of water evaporated}}{\text{energy used}}$$

SMER helps determine the effectiveness and efficiency of the drying process. A high SMER value indicates that the drying system can dehumidify quickly and effectively, while a low SMER value indicates a lower dehumidification capacity of the system.

The energy efficiency for cabinet, drying efficiency and overall energy efficiency of all systems have been examined using the following definitions [31].

Energy efficiency for cabinet

$$\eta_{\text{cabinet}} = \frac{\text{enthalpy of product}}{\text{energy used in the cabinet}} \tag{3}$$

Drying efficiency

$$\eta_{\text{drying}} = \frac{\text{enthalpy of rate of water evaporation}}{\text{energy used in the cabinet}} \tag{4}$$

Whole system efficiency

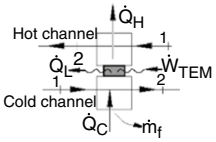
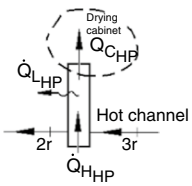
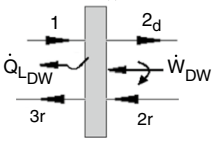
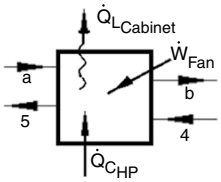
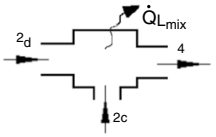
$$\eta_{\text{system}} = \frac{\text{enthalpy of rate of moisture evoparation}}{\text{energy used in the system}} \tag{5}$$

Exergy analysis applications for the models

The specific exergy of the humid air is calculated by using the following equation.

$$\begin{aligned} \text{ex}_a = {} & \left(C_a + X_a C_v\right)\left(T_a - T_0\right) - T_0\left[\left(C_a + X_a C_v\right)\ln\frac{T_a}{T_0}\right] \\ & - \left(R_a + X_a R_v\right)\ln\frac{P_a}{P_0} + T_0\left(R_a + X_a R_v\right)\ln\frac{1 + 1.6078X_0}{1 + 1.6078X_a} \\ & + 1.6078 + x_a R_a \ln\frac{x_0}{x_a} \end{aligned} \tag{6}$$

Table 1 Model-A mass, energy and exergy balance relations

Component	Mass, energy and exergy equations
TEM 	$\dot{m}_{ac1} = \dot{m}_{ac2} = \dot{m}_{ac}, \dot{m}_{ah1} = \dot{m}_{ah3} = \dot{m}_{ah}$ $\dot{m}_{ac} w_1 = \dot{m}_f + \dot{m}_{ac} w_2, \dot{m}_{ah} w_1 = \dot{m}_{ah} w_3, w_1 = w_3$ $\dot{Q}_H = \dot{m}_{ah}(h_3 - h_1), \dot{Q}_C = \dot{m}_{ac}(h_1 - h_2) - \dot{m}_f h_f, \dot{W}_{TEM} = \dot{Q}_H + \dot{Q}_C + \dot{Q}_L$ $\dot{E}_{x_{in,TEM}} = T_0\left(\frac{\dot{Q}_H}{T_H}\right), \dot{E}_{x_{out,TEM}} = T_0\left(\frac{\dot{Q}_C}{T_C}\right), \dot{E}_{x_{d,TEM}} = \dot{E}_{x_{in,TEM}} - \dot{E}_{x_{out,TEM}}$
HP 	$\dot{Q}_{H_{HP}} = \dot{Q}_{C_{HP}} + \dot{Q}_{L_{HP}}$ $\dot{E}_{x_{in,HP}} = \dot{m}_{ah} ex_{r3} - \dot{m}_{ah} ex_{r2}$ $\dot{E}_{x_{out,HP}} = \dot{Q}_{C_{HP}}\left(1 - \frac{T_0}{T_5}\right) + \dot{E}_{QL_{HP}}$ $\dot{E}_{x_{d,HP}} = \dot{E}_{x_{in,HP}} - \dot{E}_{x_{out,HP}}$
DW 	$\dot{W}_{DM} + \dot{m}_{ah}(h_{2r} - h_{3r}) + \dot{m}_{ad}(h_1 - h_{2d}) - \dot{Q}_{L_{DW}} = 0$ $\dot{E}_{x_{DM}} + \dot{m}_{ah}(ex_{2r} - ex_{3r}) + \dot{m}_{ad}(ex_1 - ex_{2d}) - \dot{E}_{x_{QL_{DW}}} = 0$
Drying cabinet 	$\dot{m}_{sa} h_{sa} + \dot{m}_{wa} h_{wa} + \dot{m}_{4mix} h_4 + \dot{W}_{Fan} + \dot{Q}_{C_{HP}} = \dot{m}_{sb} h_{sb} + \dot{m}_{wb} h_{wab} + \dot{m}_5 h_5 + \dot{Q}_{L_{cabinet}}$ $\dot{E}_{x_{in,cabinet}} = \dot{m}_{sa} ex_{sa} + \dot{m}_{wa} ex_{wa} + \dot{m}_4 ex_{4mix} + \dot{E}x_{Fan} + \dot{E}x_{QC_{HP}}$ $\dot{E}_{x_{out,cabinet}} = \dot{m}_{sb} ex_{sb} + \dot{m}_{wb} ex_{wab} + \dot{m}_5 ex_5 + \dot{E}x_{QL_{cabinet}}$ $\dot{E}_{x_{d,cabinet}} = \dot{E}_{x_{in,cabinet}} - \dot{E}_{x_{out,cabinet}}$
Mixer 	$\dot{m}_{ad} h_{2d} + \dot{m}_{ac} h_{2c} = (\dot{m}_{ac} + \dot{m}_{ad}) h_4 + \dot{Q}_{L_{mix}}$ $\dot{E}_{x_{in,mixer}} = \dot{m}_{ad} ex_{2d} + \dot{m}_{ac} ex_{2c}$ $\dot{E}_{x_{out,mixer}} = (\dot{m}_{ac} + \dot{m}_{ad}) ex_4 + \dot{E}x_{QL_{mixer}}$ $\dot{E}_{x_{d,mixer}} = \dot{E}_{x_{in,mixer}} - \dot{E}_{x_{out,mixer}}$

The specific exergy of the solid hazelnut is approximated following the equation.

$$ex_p = C_p\left[(T_p - T_o) - T_o \mathrm{Ln}\frac{T_p}{T_o}\right] \tag{7}$$

The specific exergy of the water content of the hazelnut can be approximated by using the following equation.

$$ex_w = \left[h_f(T) - h_g(T_0)\right] + \left[P - P_g(T)\right] v_f(T) - T_0\left[s_f(T) - s_g(T_0)\right] + T_0 R_v \ln\frac{P_g(T_0)}{x_{v_0}(P_0)} \tag{8}$$

The terminologies used in the literature [32] have been employed to compare the performance of considered models among themselves and for climatic conditions (climatic zone-A, climatic zone-B and climatic zone-C).

Exergy efficiency ε is a parameter that measures how effectively an energy system or process can utilize its exergy (usable energy) resources and represents the quality or usability degree of energy. Exergy efficiency ε is a parameter that measures how effectively a thermal system can utilize its energy resources and represents the quality or usability degree of energy. The exergy efficiency ε of a process is defined by the following equation.

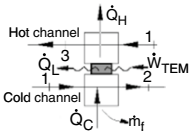
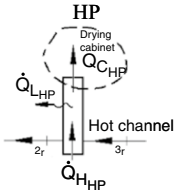
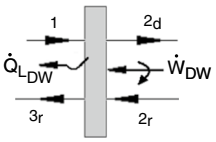
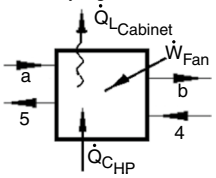
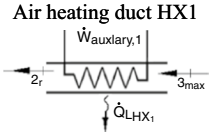
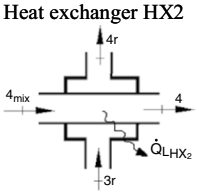
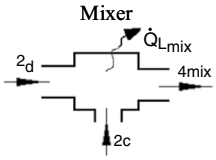
$$\varepsilon = \frac{\mathrm{Ex}_{out}}{\mathrm{Ex}_{in}} 100 \tag{9}$$

Improvement potential $I\dot{P}$ refers to the evaluation of opportunities for enhancing thermal efficiency and assessing possibilities for improvement. When the $I\dot{P}$ factor is less than 1, it indicates that the system operates effectively in terms of energy efficiency. The improvement potential of the process is defined as:

$$\dot{IP} = (1 - \varepsilon)\left(\mathrm{Ex}_{in} - \mathrm{Ex}_{out}\right) \tag{10}$$

Exergetic factor f_i is a parameter in thermal systems that represents the quality loss of energy conversion processes

Table 2 Model-B mass, energy and exergy balance relations

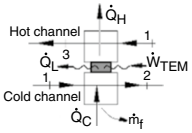
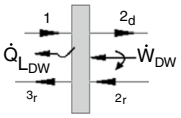
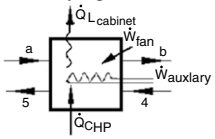
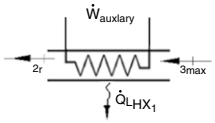
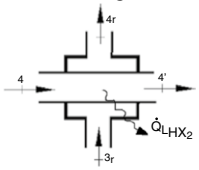
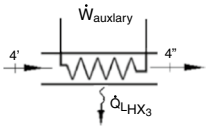
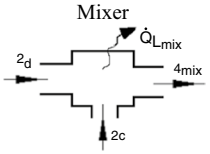
Component	Mass, energy and exergy equations
TEM 	$\dot{m}_{ac1} = \dot{m}_{ac2} = \dot{m}_{ac}, \dot{m}_{ah1} = \dot{m}_{ah3} = \dot{m}_{ah}$ $\dot{m}_{ac} w_1 = \dot{m}_f + \dot{m}_{ac} w_2, \dot{m}_{ah} w_1 = \dot{m}_{ah} w_3, w_1 = w_3$ $\dot{Q}_H = \dot{m}_{ah}(h_3 - h_1), \dot{Q}_C = \dot{m}_{ac}(h_1 - h_2) - \dot{m}_f h_f, \dot{W}_{TEM} = \dot{Q}_H + \dot{Q}_C + \dot{Q}_L$ $\dot{E}_{x_{in,TEM}} = T_0\left(\frac{\dot{Q}_H}{T_H}\right), \dot{E}_{x_{out,TEM}} = T_0\left(\frac{\dot{Q}_C}{T_C}\right), \dot{E}_{x_{d,TEM}} = \dot{E}_{x_{in,TEM}} - \dot{E}_{x_{out,TEM}}$
HP 	$\dot{Q}_{H_{HP}} = \dot{Q}_{C_{HP}} + \dot{Q}_{L_{HP}}$ $\dot{E}_{x_{in,HP}} = \dot{m}_{ah} ex_{r3} - \dot{m}_{ah} ex_{r2}$ $\dot{E}_{x_{out,HP}} = \dot{Q}_{C_{HP}}\left(1 - \frac{T_0}{T_m}\right) + \dot{E}_{QL_{HP}}$ $\dot{E}_{x_{d,HP}} = \dot{E}_{x_{in,HP}} - \underset{out,HP}{Ex}$
DW 	$\dot{W}_{DM} + \dot{m}_{ah}(h_{2r} - h_{3r}) + \dot{m}_{ad}(h_1 - h_{2d}) - \dot{Q}_{L_{DW}} = 0$ $\dot{E}_{x_{DM}} + \dot{m}_{ah}(ex_{2r} - ex_{3r}) + \dot{m}_{ad}(ex_1 - ex_{2d}) - \dot{E}_{x_{QL_{DW}}} = 0$
Drying cabinet 	$\dot{m}_{sa} h_{sa} + \dot{m}_{wa} h_{wa} + \dot{m}_4 h_{4mix} + \dot{W}_{Fan} + \dot{Q}_{C_{HP}} = \dot{m}_{sb} h_{sb} + \dot{m}_{wb} h_{wab} + \dot{m}_5 h_5 + \dot{Q}_{L_{cabinet}}$ $\dot{E}_{x_{in,cabinet}} = \dot{m}_{sa} ex_{sa} + \dot{m}_{wa} ex_{wa} + \dot{m}_4 ex_4 + \underset{Fan}{Ex} + \underset{QC_{HP}}{Ex}$ $\dot{E}_{x_{out,cabinet}} = \dot{m}_{sb} ex_{sb} + \dot{m}_{wb} ex_{wab} + \dot{m}_5 ex_5 + \dot{E}x_{QL_{cabinet}}$ $\dot{E}_{x_{d,cabinet}} = \dot{E}_{x_{in,cabinet}} - \dot{E}_{x_{out,cabinet}}$
Air heating duct HX1 	$\dot{W}_{Auxlary,1} + (\dot{m}_{ah}) h_{3max} = (\dot{m}_{ah}) h_{2r} + \dot{Q}_{L_{HX1}}$ $\dot{E}_{x_{in,HX1}} = \dot{E}_{x_{Auxlary}} + (\dot{m}_{ah}) ex_{3max}$ $\dot{E}_{x_{out,HX1}} = \dot{E}_{x_{QL-HX1}} + (\dot{m}_{ah}) ex_{2r}$ $\dot{E}_{x_{d,HX1}} = \dot{E}_{x_{in,HX1}} - \dot{E}_{x_{out,HX1}}$
Heat exchanger HX2 	$(\dot{m}_{ac} + \dot{m}_{ad}) h_{4mix} + \dot{m}_{ah} h_{3r} = (\dot{m}_{ac} + \dot{m}_{ad}) h_4 + (\dot{m}_{ac} + \dot{m}_{ad}) h_{4r} + \dot{Q}_{L_{HX2}}$ $\dot{E}_{x_{in,HX2}} = (\dot{m}_{ac} + \dot{m}_{ad}) ex_{4mix} + \dot{m}_{ah} ex_{3r}$ $\dot{E}_{x_{out,HX2}} = (\dot{m}_{ac} + \dot{m}_{ad}) ex_4 + (\dot{m}_{ac} + \dot{m}_{ad}) ex_{4r} + \dot{E}_{x_{QL_{HX2}}}$ $\dot{E}_{x_{d,HX2}} = \dot{E}_{x_{in,HX2}} - \dot{E}_{x_{out,HX2}}$
Mixer 	$\dot{m}_{ad} h_{2d} + \dot{m}_{ac} h_{2c} = (\dot{m}_{ac} + \dot{m}_{ad}) h_{4mix} + \dot{Q}_{L_{mix}}$ $\dot{E}_{x_{in,mixer}} = \dot{m}_{ad}\, ex_{2d} + \dot{m}_{ac}\, ex_{2c}$ $\dot{E}_{x_{out,mixer}} = (\dot{m}_{ac} + \dot{m}_{ad}) ex_{4mix} + \dot{E}_{x_{QL_{mixer}}}$ $\dot{E}_{x_{d,mixer}} = \dot{E}_{x_{in,mixer}} - \dot{E}_{x_{out,mixer}}$

and indicates the portion of energy in a system that is conserved as exergy (usable energy). Exergetic factor f_i is defined in the following equation.

$$f_i = \frac{\dot{F}_i}{\dot{F}_{total}} 100 \tag{11}$$

where $\dot{F}_i$ is the rate of the exergy of the fuel, and $\dot{F}_{total}$ is the submission of the exergy of the fuel inlet of the component. The sustainability index (SI) is a parameter used to objectively measure the sustainability performance of thermal systems and guide decision-making processes. When the SI factor is greater than 1, it indicates that the system utilizes energy sources effectively. The sustainability index (SI) is given by.

Table 3 Model-C mass, energy and exergy balance relations

Component	Mass, energy and exergy equations
TEM 	$\dot{m}_{ac1} = \dot{m}_{ac2} = \dot{m}_{ac}, \dot{m}_{ah1} = \dot{m}_{ah3} = \dot{m}_{ah}$ $\dot{m}_{ac} w_1 = \dot{m}_f + \dot{m}_{ac} w_2, \dot{m}_{ah} w_1 = \dot{m}_{ah} w_3, w_1 = w_3$ $\dot{Q}_H = \dot{m}_{ah}(h_3 - h_1), \dot{Q}_C = \dot{m}_{ac}(h_1 - h_2) - \dot{m}_f h_f, \dot{W}_{TEM} = \dot{Q}_H + \dot{Q}_C + \dot{Q}_L$ $\dot{E}_{x_{in,TEM}} = T_0\left(\frac{\dot{Q}_H}{T_H}\right), \dot{E}_{x_{out,TEM}} = T_0\left(\frac{\dot{Q}_C}{T_C}\right), \dot{E}_{x_{d,TEM}} = \dot{E}_{x_{in,TEM}} - \dot{E}_{x_{out,TEM}}$
DW 	$\dot{W}_{DM} + \dot{m}_{ah}(h_{2r} - h_{3r}) + \dot{m}_{ad}(h_1 - h_{2d}) - \dot{Q}_{L_{DW}} = 0$ $\dot{E}_{x_{DM}} + \dot{m}_{ah}(ex_{2r} - ex_{3r}) + \dot{m}_{ad}(ex_1 - ex_{2d}) - \dot{E}_{x_{QL_{DW}}} = 0$
Drying cabinet 	$\dot{m}_{sa} h_{sa} + \dot{m}_{wa} h_{wa} + \dot{m}_{4mix} h_{4mix} + \dot{W}_{fan} + \dot{W}_{auxlary} + \dot{Q}_{C_{HP}} = \dot{m}_{sb} h_{sb} + \dot{m}_{wb} h_{wab} + \dot{m}_5 h_5 + \dot{Q}_{L_{cabinet}}$ $\dot{E}_{x_{in,cabinet}} = \dot{m}_{sa}\, ex_{sa} + \dot{m}_{wa}\, ex_{wa} + \dot{m}_{4mix}\, ex_{4mix} + \dot{E}x_{fan} + \dot{E}x_{QC_{HP}} + \dot{E}x_{auxlary}$ $\dot{E}_{x_{out,cabinet}} = \dot{m}_{sb}\, ex_{sb} + \dot{m}_{wb}\, ex_{wab} + \dot{m}_5\, ex_5 + \dot{E}x_{QL_{cabinet}}$ $\dot{E}_{x_{d,cabinet}} = \dot{E}_{x_{in,cabinet}} - \dot{E}_{x_{out,cabinet}}$
Air heating duct HX1 	$\dot{W}_{Auxlary,1} + (\dot{m}_{ac} + \dot{m}_{ad}) h_{3max} = (\dot{m}_{ac} + \dot{m}_{ad}) h_{2r} + \dot{Q}_{L_{HX1}}$ $\dot{E}_{x_{in,HX1}} = \dot{E}_{x_{Auxlary}} + (\dot{m}_{ac} + \dot{m}_{ad}) ex_{3max}$ $\dot{E}_{x_{out,HX1}} = \dot{E}_{x_{QL-HX1}} + (\dot{m}_{ac} + \dot{m}_{ad}) ex_{2r}$ $\dot{E}_{x_{d,HX1}} = \dot{E}_{x_{in,HX1}} - \dot{E}_{x_{out,HX1}}$
Heat exchanger HX2 	$(\dot{m}_{ac} + \dot{m}_{ad}) h_4 + \dot{m}_{ah} h_{3r} = (\dot{m}_{ac} + \dot{m}_{ad}) h_{4'} + (\dot{m}_{ah}) h_{4r} + \dot{Q}_{L_{HX2}}$ $E_{x_{in,HX2}} = (\dot{m}_{ac} + \dot{m}_{ad}) ex_4 + \dot{m}_{ah} ex_{3r}$ $\dot{E}_{x_{out,HX2}} = (\dot{m}_{ac} + \dot{m}_{ad}) ex h_{4'} + (\dot{m}_{ah}) ex_{4r} + \dot{E}_{x_{QL-HX2}}$ $\dot{E}_{x_{d,HX2}} = \dot{E}_{x_{in,HX2}} - \dot{E}x_{ouut,HX2}$
Air heating duct HX3 	$\dot{W}_{Auxlary,3} + (\dot{m}_{ac} + \dot{m}_{ad}) h_{4'} = (\dot{m}_{ac} + \dot{m}_{ad}) h_{4''} + \dot{Q}_{L_{HX3}}$ $E_{x_{in,HX3}} = \dot{W}_{Auxlary,3} + (\dot{m}_{ac} + \dot{m}_{ad}) ex_{4'}$ $E_{x_{out,HX3}} = (\dot{m}_{ac} + \dot{m}_{ad}) ex_{4''} + \dot{Q}_{L_{HX3}}$ $\dot{E}_{x_{d,HX3}} = \dot{E}_{x_{in,HX3}} - \dot{E}_{x_{out,HX3}}$
Mixer 	$\dot{m}_{ad} h_{2d} + \dot{m}_{ac} h_{2c} = (\dot{m}_{ac} + \dot{m}_{ad}) h_{4mix} + \dot{Q}_{L_{mix}}$ $\dot{E}_{x_{in,mixer}} = \dot{m}_{ad} ex_{2d} + \dot{m}_{ac} ex_{2c}$ $\dot{E}_{x_{out,mixer}} = (\dot{m}_{ac} + \dot{m}_{ad}) ex_{4mix} + \dot{E}_{x_{QL_{mixer}}}$ $\dot{E}_{x_{d,mixer}} = \dot{E}_{x_{in,mixer}} - \dot{E}_{x_{out,mixer}}$

$$SI = \frac{1}{1 - \eta_{ex}} \tag{12}$$

Relative irreversibility is a parameter that indicates how inefficient a thermal system or process is and quantifies the amount of energy loss. Relative irreversibility is defined in Eq. (13).

$$RI = \frac{\dot{E}_{x_{d,k}}}{\dot{E}_{x_{d,total}}} 100 \tag{13}$$

where $\dot{E}x_{d,k}$ is the exergy destruction at the kth component, and $\dot{E}x_{d,total}$ is the total exergy inflow in the system.

Exergy destruction for TEM is calculated concerning [14]. The mass balance, energy and exergy balance equations for each component of Model-A and Model-B and Model-C are given in Table 1–3.

Table 4 The results of the energy analysis for all models

T_{apd}/°C	$W_{elektrik}$/kW	SMER/kg-H_2O k Wh^{-1}	Total energy cost/$	Unit Energy cost/ kg-H_2OkWh^{-1}	The unit cost of the product/$ kg^{-1}-nut	Drying Process efficiency/%	Energy efficient/%	Whole syste efficiency/%	Drying air-specific humidity gr-H_2O kg^{-1}-dry air	Drying air relative humidity %
Model-A (T_{db} = 38 °C, RH = 85%)										
24	1.47	0.271	11.36	0.106	0.11	4.58	4.66	18.20	21.0	45
Model-B (T_{db} = 30 °C, RH = 75%)										
19	2.61	0.1542	20.03	0.106	0.199	10.35	9.87	10.35	17.5	58
Model-C (T_{db} = 23.5 °C, RH = 70%)										
12	2.69	0.1381	22.37	0.106	0.205	8.31	9.13	8.35	9.0	38

Results and discussion

The thermodynamic analysis results of the three different models were summarized and are presented in Table 4, in the study. In all three models, it has been observed that the specific humidity and relative humidity of the drying air for the product attain significantly reduced levels compared to the specific humidity and relative humidity of the atmospheric air. The energy-based cost per unit product quantity was determined as 0.11 $\$kg^{-1}$-nut for Model-A, 0.199 $\$kg^{-1}$-nut for Model-B and 0.205 $\$kg^{-1}$-nut for Model-C in the three models. The electricity energy cost for the year 2023 is 0.106 US dollars per kilowatt-hour in Türkiye. Evaluation of performance parameters of the models based on apparatus dew point temperature variation in the study is presented in Table 5.

When examining Figs. 7–9, it is observed that maintaining a significant difference between the atmospheric air dew point temperature and the applied T_{apd} temperature results in an improvement in energy efficiency and exergy efficiency of the models.

According to Table 6 in the study, among the models designed according to climatic zone conditions, Model-C exhibits the highest energy demand and cost. Due to the low specific humidity of the outlet air from the drying chamber in Model-C, its efficiency can be enhanced when used in conjunction with another system. Additionally, Model-C has the potential to reduce drying time, thereby enabling energy savings on its own. This aspect can be considered another factor that enhances the energy efficiency of Model-C.

Upon examining Table 5, it has been determined that in all models, as the apparatus dew point temperature increases, the electrical power applied to the TEM element and the mass flow rate of the drying air entering the cabinet increase. Furthermore, in all models, as the apparatus dew point temperature increases, the exergy of the air at the inlet of the cabinet is observed to increase. For all models, it was found that at the apparatus dew point temperature limits, the exergy efficiency ε_{system} of Model-A remains approximately 62%, while in Model-B it is 22% and in Model-C it is 10.1%. Additionally, as the apparatus dew point temperature increases, it was obtained that the drying process efficiency, energy efficiency, whole system efficiency and SMER decrease in all models. It has been observed that in Model-C, the energy input to the drying air is higher than that in Model-A and Model-B, resulting in Model-C having the lowest drying process efficiency value of 3.42.

The comparison of the energy efficiency of some different hybrid dryers reported in the literature and the models considered in the study is presented in Table 6.

The SMER values of the models considered in the study for hazelnut drying present acceptable results when

Table 5 Evaluation of performance parameters of the models based on apparatus dew point temperature variation

T_{apd} (°C)	$\dot{m}_{air,in,cabinet}$/kg s^{-1}	ε_{system}/%	Drying process efficiency/%	Energy efficient/%	Whole system efficiency/%	$ex_1 * \dot{m}_{a,in,\ cabinet}$ /kW	SMER/kg-H_2OkWh^{-1}	$\dot{W}_{TEM}$/kW
Model-A								
20	0.0438	61.93	4.76	4.84	18.26	0.0384	0.2726	1.467
24	0.0453	62.18	4.58	4.66	18.20	0.0397	0.2717	1.470
26	0.0466	62.37	4.44	4.52	18.02	0.0409	0.269	1.487
29	0.0503	62.86	4.11	4.18	17.30	0.044	0.2582	1.55
32	0.0613	63.98	3.35	3.41	15.03	0.0537	0.224	1.78
Model-B								
17	0.0159	22.49	12.01	12.77	10.74	0.010	0.1510	1.618
19	0.0305	22.43	10.25	10.89	10.35	0.116	0.1533	1.670
21	0.0387	22.32	7.93	8.43	9.54	0.0147	0.1413	1.823
23	0.0629	22.068	4.76	5.064	7.62	0.0239	0.1129	2.286
Model-C								
10	0.0399	10.94	9.86	10.83	8.89	0.0049	0.1308	2.0
12	0.0469	10.77	8.31	9.13	8.35	0.0058	0.1229	2.11
14	0.0615	10.51	6.25	6.87	7.30	0.0076	0.1074	2.375
16	0.1105	10.03	3.42	3.75	5.03	0.0137	0.074	3.31

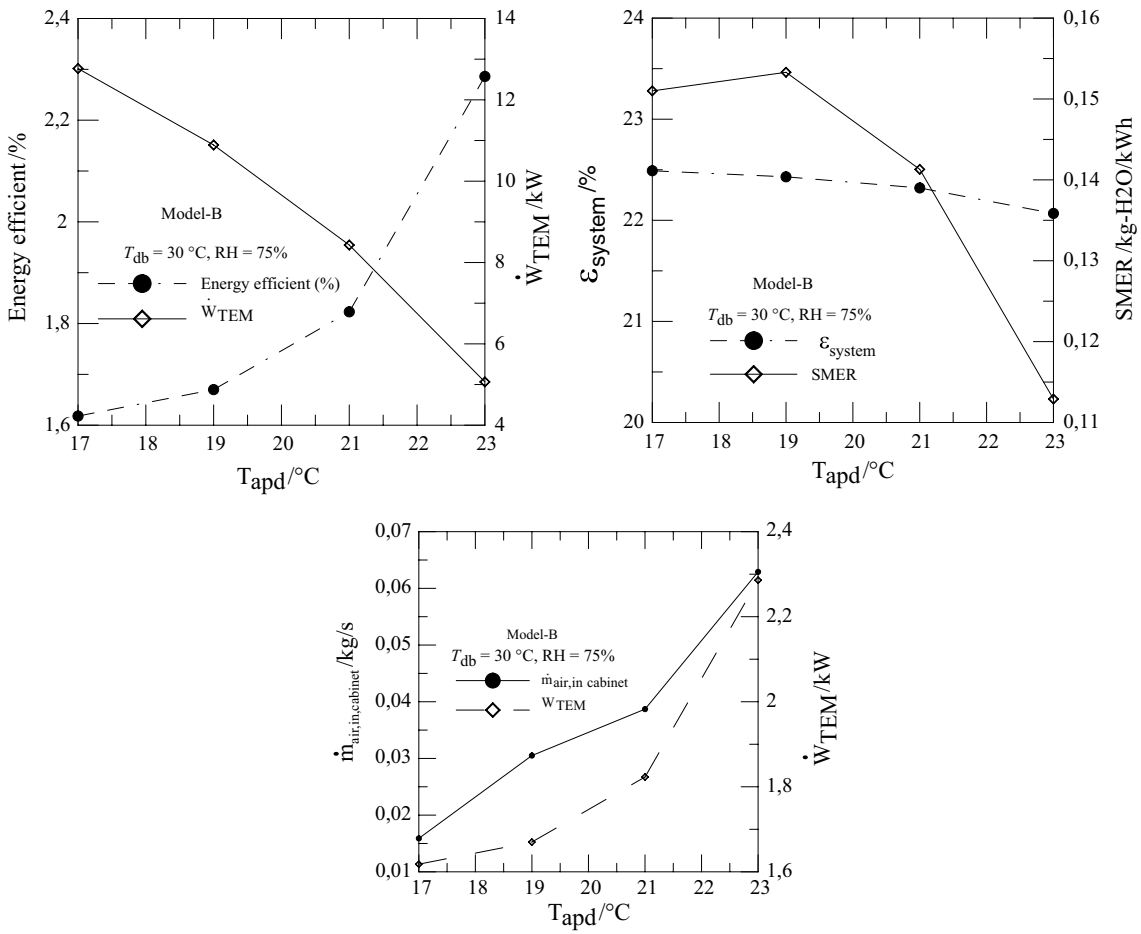


Fig. 7 The variation of performance parameters of Model-B with respect to T_{apd} temperature

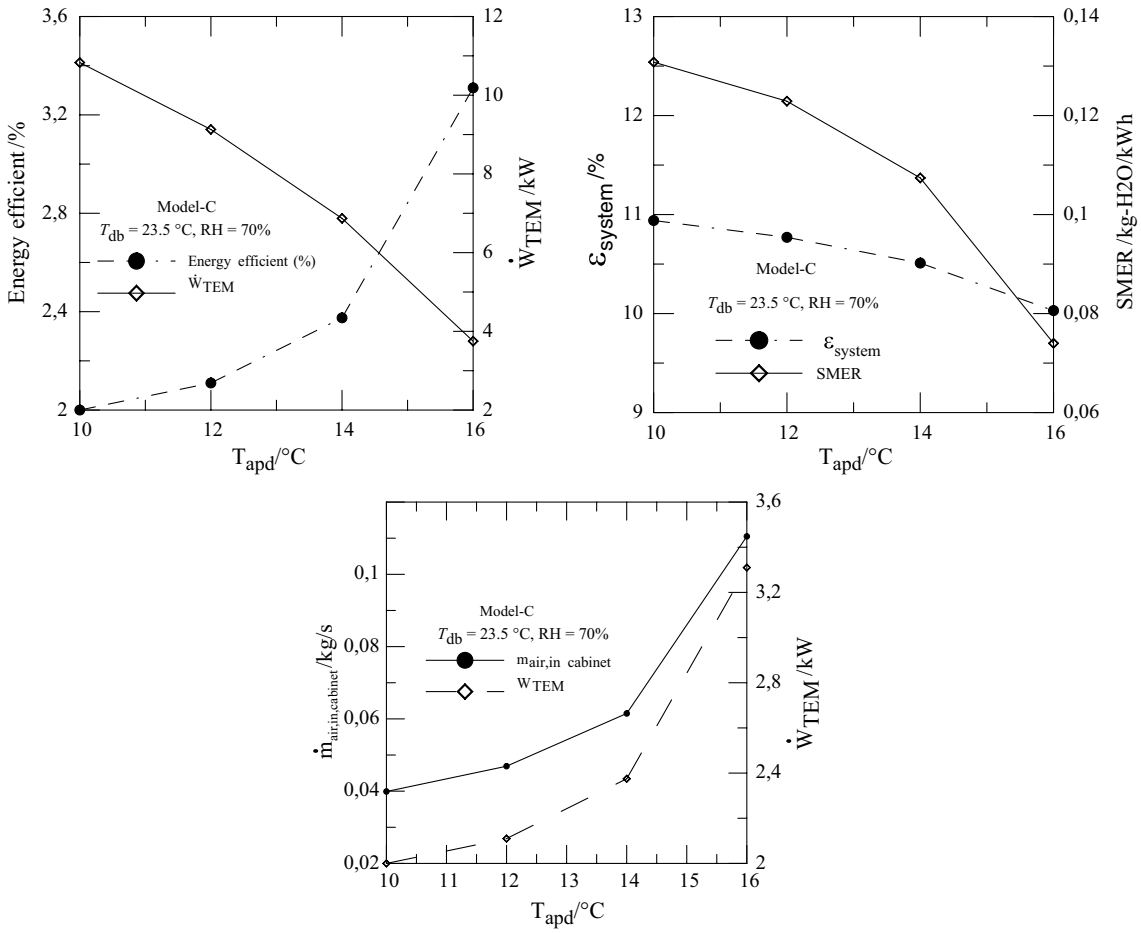


Fig. 8 The variation of performance parameters of Model-C with respect to T_{apd} temperature

compared with the literature values in Table 6. Furthermore, despite the lower SMER values of the models compared to the literature data due to maintaining the drying air temperature at 43 °C based on the climatic zones, the introduced models demonstrate the potential for reducing the drying time and increasing the SMER value. This table presents the quantitative values of the impact of climatic conditions on the presented models. When comparing the results obtained from the models with the set of results presented in the literature, it is evident that the models demonstrate their applicability.

The exergy analysis results were obtained based on the selected dew point temperatures in Model-A, Model-B and Model-C, considering the approximate energy values relative to the average values of the required energies in the TEM element. The exergy analysis results for the three models are presented in Table 7.

When Fig. 9 is examined, the Model-A was also identified in the largest exergy destroying TEM component, and the Model-B in HX1 and Model-C in TEM and HX1 components.

Table 7 presents the calculated SI values of the system components in the models. The high SI values of the system components indicate a combination of high efficiency and low environmental impact. The SI values of the systems are used in all three models, and it has been observed that are higher than 1.0 units. In all three models, the highest variation in SI values, attributed to decreasing ambient temperature, was observed in the DW component (1.76 in Model-A, 10.36 in Model-B and 7.58 in Model-C). TEM component exhibited varying SI values based on the cycles implemented in the models (Model-A, 4.34, Model-B, 5.149, and Model-C, 4.41).

It can be observed from Table 7 that the TEM component has the highest values of the exergetic factor (*f*) in all three models. This indicates that a significant portion of the system exergy is utilized by the TEM component. The exergetic factors (*f*) for the drying chamber are lower than those of the TEM component in all three models.

When comparing the exergetic efficiencies (ε) of the system components, it was found that the highest ε values were observed for the DW and TEM components in all models. ε

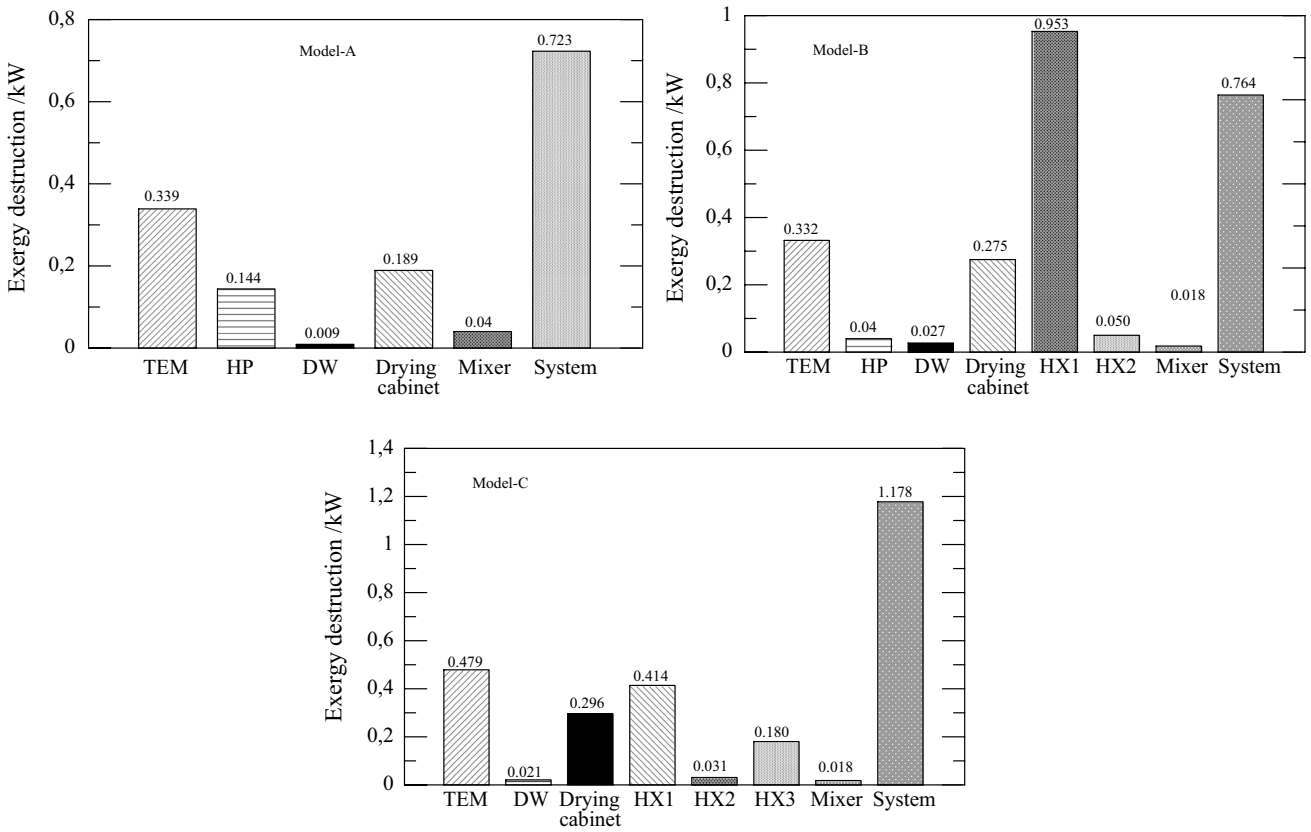


Fig. 9 Exergy destruction distribution of components in models

Table 6 The comparison of the energy efficiency and the SMER index obtained in the study with some studies reported in the literature

Type of drying	Drying sample	Energy efficiency	SMER	References
Hot air + Solar drying	Tomato	17–29	–	[33]
Heat pump + photovoltaic thermal dryer	Saffron	10.8–72	–	[34]
Solar + thermal shelf	Black turmeric	12	–	[35]
Heat pump	Green sweet pepper	–	0.55–1.1	[36]
Heat pump	Ginger	–	0.26–0.47	[37]
Heat pump	Mushroom	–	0.26–0.92	[38]
Model-A	Hazel nut	18.20	0.271	Present study
Model-B	Hazel nut	10.35	0.153	Present study
Model-C	Hazel nut	8.35	0.122	Present study

for the drying cabinet was found to be 21.06% in Model-A, 12.59% in Model-B and 16.88% in Model-C. Maintaining the drying air temperature at 43 °C at the inlet of the drying cabinet under chosen climatic zone conditions caused variations in the ε of the drying cabinet.

The obtained IP values for the drying cabinet in all three models are determined as 0.149, 0.240 and 0.246, respectively. These values indicate the need for improvements in the drying cabinet. However, the optimization of the relationship between cabinet dimensions and product quantities was not evaluated in this study. Optimizing these factors can contribute to reducing IP values.

The highest RI value is obtained in the TEM component in the models, while the lowest RI value is obtained in the DW component. Additionally, the high RI value observed in the air heating ducts is due to the improper selection of the component's actual dimensions.

Table 7 Results of exergy analysis for the three models

Models	Combination	Ex_{in}/kW	Ex_{out}/kW	Ex_d/kW	η_{ex}/%	*f*/%	$\dot{I}P$/kW	RI/%	SI
A	TEM	0.688	0.349	0.339	76.96	49.03	0.078	46.83	4.34
	HP	0.301	0.1557	0.144	52.23	21.45	0.068	19.89	2.093
	DW	0.113	0.1035	0.009	91.50	8.054	0.001	1.243	11.76
	Drying Cabinet	0.240	0.050	0.189	21.06	17.10	0.149	26.11	1.266
	Mixer	0.061	0.021	0.040	34.63	4.374	0.0263	5.526	1.52
	System	1.405	0.682	0.723	62.18	100	0.295	100	2.307
B	TEM	0.776	0.450	0.332	80.57	31.02	0.063	29.09	5.149
	HP	0.660	0.253	0.040	38.3	26.38	0.250	3.505	1.62
	DW	0.286	0.259	0.027	90.34	11.43	0.002	2.366	10.36
	Drying cabine t	0.315	0.039	0.275	12.59	12.59	0.240	24.10	1.14
	Air heating duct HX1	1.150	0.197	0.953	17.16	9.276	0.789	83.52	1.20
	Heat exchanger HX2	0.192	0.140	0.05	72.81	7.676	0.014	4.382	3.67
	Mixer	0.040	0.022	0.018	55	1.599	0.008	1.577	2.23
	System	2.528	1.764	0.764	22.43	100	1.530	100	1.280
C	TEM	1.052	0.572	0.479	77.32	41.96	0.108	33.19	4.41
	DW	0.166	0.144	0.021	86.8	6.621	0.002	1.455	7.58
	Drying cabinet	0.356	0.060	0.296	16.88	14.20	0.246	20.51	1.20
	Air heating duct HX1	0.507	0.092	0.414	18.27	20.22	0.339	28.69	1.22
	Heat exchanger HX2	0.062	0.030	0.031	49.20	2.473	0.016	2.148	1.96
	Heat exchanger HX3	0.338	0.158	0.180	46.7	13.48	0.096	12.47	1.87
	Mixer	0.026	0.086	0.018	31.98	1.037	0.012	1.247	1.47
	System	2.271	1.092	1.178	10.77	100	2.580	100	1.12

Conclusions

In this study, the comparison criterion among the models that comply with different temperature and humidity conditions provided by the climate zones (climatic zone-A, climatic zone-B and climatic zone-C) was primarily based on the drying cabinet.

When the cycles of these three models are examined in the psychometric diagram, the advantages of the cycles are listed as follows:

1. In chosen climatic zone conditions, the specific humidity of the cabin supply air at a dry bulb temperature of 43 °C has been determined as 0.022 kg-H_2Okg^{-1}-dry air for Model-A, 0.018 kg-H_2Okg^{-1}-dry air for Model-B and 0.014 kg-H_2Okg^{-1}-dry air for Model-C. Due to the significantly lower specific humidity values of the cabin supply air compared to atmospheric air, increasing the air's saturation level in the models will accelerate the drying process of hazelnuts in the models. This finding is particularly evident in Model-C. The reduction in drying time indicates that the SMER values associated with the models can increase based on climatic zone temperatures. This observation suggests a decrease in energy consumption and cost for hazelnut drying.
2. When the cabin outlet air is maintained at a constant temperature of 40 °C, its specific humidity is significantly lower than the specific humidity values of the selected climatic zone air. This situation allows for the possibility of reusing the cabin outlet drying air with minimal energy consumption, thereby increasing the SMER value of the new system.
3. In the conducted study, the efficiencies and SEMER (solar energy conversion efficiency) values of Model-A, Model-B and Model-C were provided based on atmospheric conditions. Each model is valid under its characteristic operating conditions. The energy efficiencies and SEMER values for Model-A, Model-B and Model-C were determined as 4.66%-0.271 kg-H_2OkWh^{-1}, 9.87%-0.1542 kg-H_2OkWh^{-1} and 9.13%-0.1381 kg-H_2OkWh^{-1}, respectively.
4. The high SI values of the introduced models provide a roadmap for achieving sustainability goals in the energy sector and enable the balanced evaluation of the environmental, economic, and social impacts of energy systems. The presented models of hazelnut drying supported by renewable energy have achieved high SI values. Consequently, these models ensure the sustainability of energy in the drying sector and facilitate the assessment of their environmental, economic and social impacts. The utilization of renewable energy in the models will lead to a reduction in CO_2 emissions during the drying process.
5. The Model-A, with a system IP value of 0.295 indicating energy efficiency and a system SI value of 2.307 indicat-

ing effective utilization of energy resources, has been found to be more suitable compared to other models in terms of energy efficiency.

For future studies, it is recommended to investigate the impact of variables such as air mass flow rate, product loading density, apparatus dew point temperature and system sizes on the exergy efficiency of the entire system for all three models.

Author contributions Each author contributed significantly to the development and writing of this paper. The specific contributions of each author are outlined below: [BS]: The author performed thermodynamic calculations for the models in the paper. [CD]: The author conducted a literature review and compiled the relevant information for the paper. [TA]: The author translated the paper into English. All authors have read and approved the final version of the manuscript.

Funding Open access funding provided by the Scientific and Technological Research Council of Türkiye (TÜBİTAK).

Declarations

Conflict of interest Authors declare that they have no conflict of interest.

Open Access This article is licensed under a Creative Commons Attribution 4.0 International License, which permits use, sharing, adaptation, distribution and reproduction in any medium or format, as long as you give appropriate credit to the original author(s) and the source, provide a link to the Creative Commons licence, and indicate if changes were made. The images or other third party material in this article are included in the article's Creative Commons licence, unless indicated otherwise in a credit line to the material. If material is not included in the article's Creative Commons licence and your intended use is not permitted by statutory regulation or exceeds the permitted use, you will need to obtain permission directly from the copyright holder. To view a copy of this licence, visit http://creativecommons.org/licenses/by/4.0/.

References

1. Ceylan I, Ergun A. Psychometric analysis of a timber dryer. Case Stud Therm Eng. 2014;2:29–35. https://doi.org/10.1016/j.csite.2013.11.003.
2. Pandey M, Acharya SK, Mishra I, Drying of chili using solar cabinet dryer & analysis with results of various parameters, (n.d.). www.ijraset.com.
3. Ye L, Mesery HS, Ashfaq MM, Shi Y, Zicheng H, Alshaer WG. Analysis of energy and specific energy requirements in various drying process of mint leaves. Case Stud Therm Eng. 2021;26:101113. https://doi.org/10.1016/j.csite.2021.101113.
4. Akbulut A, Durmuş A. Energy and exergy analyses of thin layer drying of mulberry in a forced solar dryer. Energy. 2010;35:1754–63. https://doi.org/10.1016/j.energy.2009.12.028.
5. Caliskan H, Lee DY, Hong H. Enhanced thermodynamic assessments of the novel desiccant air cooling system for sustainable energy future. J Clean Prod. 2019;211:213–21. https://doi.org/10.1016/j.jclepro.2018.11.174.
6. Saraç B. Thermodynamic analysis of the availability of dehumidifier and evaporation-cooled air conditioning systems in tea factories. DEU Eng Fac Sci Eng J. 2017;19:927–37. https://doi.org/10.21205/deufmd.2017195781.
7. Saraç B. Thermodynamic analysis of drying evaporative cooling systems defined for ro-ro cargo ship. Deu Eng Fac Sci Eng J. 2019;21:733–40. https://doi.org/10.21205/deufmd.2019216305.
8. Saraç B, Aksu E, Ayhan T, Effects of reversions in an ambient air cooling processes on blowing air exergy value limits. in: SETSCI conference proceedings. 2019, pp. 1–6. https://doi.org/10.36287/setsci.4.6.007.
9. Gungor A, Erbay Z, Hepbasli A. Exergetic analysis and evaluation of a new application of gas engine heat pumps (GEHPs) for food drying processes. Appl Energy. 2011;88:882–91. https://doi.org/10.1016/j.apenergy.2010.09.007.
10. Giannetti N, Yamaguchi S, Rocchetti A, Saito K. Thermodynamic analysis of irreversible desiccant systems. Entropy. 2018;20:595. https://doi.org/10.3390/e20080595.
11. Rafique MM, Gandhidasan P, Al-Hadhrami LM, Rehman S. Energy exergy and anergy analysis of a solar desiccant cooling system. J Clean Energy Technol. 2015;4:78–83. https://doi.org/10.7763/jocet.2016.v4.257.
12. Kulkarni KK, Shinde VS. Thermodynamic analysis of desiccant assisted hybrid air conditioning system. Int Eng Res J. 2015;2:4902–5.
13. Patel KK, Kar A. Heat pump assisted drying of agricultural produce-an overview. J Food Sci Technol. 2012;49:142–60. https://doi.org/10.1007/s13197-011-0334-z.
14. Sharma S, Dwivedi VK, Pandit SN. Exergy analysis of single-stage and multi stage thermoelectric cooler. Int J Energy Res. 2014;38:213–22. https://doi.org/10.1002/er.3043.
15. Kara O, Hürdoğan E, Kula S, Büyükalaca O. Second law analysis of an adsorption air-conditioning system. Cumhur Sci J. 2016;37:131. https://doi.org/10.17776/csj.80854.
16. Khalifa AJN, Al-Dabagh AM, Al-Mehemdi WM. An experimental study of vegetable solar drying systems with and without auxiliary heat. ISRN Renew Energy. 2012;2012:1–8. https://doi.org/10.5402/2012/789324.
17. Kuzgunkaya EH, Hepbasli A. Exergetic evaluation of drying of laurel leaves in a vertical ground-source heat pump drying cabinet. Int J Energy Res. 2007;31:245–58. https://doi.org/10.1002/er.1245.
18. Akpinar EK. Drying of mint leaves in a solar dryer and under open sun: modelling, performance analyses. Energy Convers Manag. 2010;51:2407–18. https://doi.org/10.1016/j.enconman.2010.05.005.
19. Colak N, Kuzgunkaya E, Hepbasli A. Exergetic assessment of drying of mint leaves in a heat pump dryer. J Food Process Eng. 2008;31:281–98. https://doi.org/10.1111/j.1745-4530.2007.00155.x.
20. la Gómez-de Cruz FJ, Palomar-Torres A, Palomar-Carnicero JM, Cruz-Peragón F. Energy and exergy analysis during drying in rotary dryers from finite control volumes: applications to the drying of olive stone. Appl Therm Eng. 2022;200:117699. https://doi.org/10.1016/j.applthermaleng.2021.117699.
21. Peinado D, De Vega M, García-Hernando N, Marugán-Cruz C. Energy and exergy analysis in an asphalt plant's rotary dryer. Appl Therm Eng. 2011;31:1039–49. https://doi.org/10.1016/j.applthermaleng.2010.11.029.
22. Luo J, Morosuk T, Tsatsaronis G, Tashtoush B. Exergetic and economic evaluation of a transcritical heat-driven compression refrigeration system with CO2 as the working fluid under hot climatic conditions. Entropy. 2019;21:1164. https://doi.org/10.3390/e21121164.
23. Dincer I, Sahin AZ. A new model for thermodynamic analysis of a drying process. Int J Heat Mass Transf. 2004;47:645–52. https://doi.org/10.1016/j.ijheatmasstransfer.2003.08.013.

24. Bardant TB, Haq MS, Setiawan AAR, Harianto S, Waluyo J, Mastur AI, Lestari AD, Sujarwo, Sulaswatty A, Wiloso EI. The renewability indicator and cumulative degree of perfection for gamboeng tea; Part.1, exergy calculation of fresh tea leaf. in: E3S web of conferences, EDP Sciences, 2018. https://doi.org/10.1051/e3sconf/20187407003.
25. Coskun C, Bayraktar M, Oktay Z, Dincer I. Energy and exergy analyses of an industrial wood chips drying process. Int J Low-Carbon Technol. 2009;4:224–9. https://doi.org/10.1093/ijlct/ctp024.
26. Hossain MZ, Alam MM, Bin Hossain MF, Sarker MSH, Awal MA, Jahan N. Performance evaluation of a cabinet solar dryer for drying red pepper in Bangladesh. J Agric Eng. 2018;49:100–9. https://doi.org/10.4081/jae.2018.774.
27. Demirtaş C. Phd thesis. Determination of Hazelnut drying conditions. Karadeniz Technical University, Institute of Natural Sciences, Department of Mechanical Engineering. Trabzon, Türkiye, 1996.
28. Krokida MK, Karathanos VT, Maroulis ZB, Marinos-Kouris D. Drying kinetics of some vegetables. J Food Eng. 2003;59:391–403. https://doi.org/10.1016/S0260-8774(02)00498-3.
29. Aksu E, Sarac B, Ayhan T. Experimental investigation and computational fluid dynamics analysis of flow and heat transfer for heated plate. J Thermophys Heat Trans. 2017;31:937–46. https://doi.org/10.2514/1.T5120.
30. Baheta AT, Looi KK, Oumer AN, Habib K. Thermoelectric air-conditioning system: building applications and enhancement techniques. Int J Air-Cond Refrig. 2019;27:19300027. https://doi.org/10.1142/S2010132519300027.
31. Menon A, Stojceska V, Tassou SA. A systematic review on the recent advances of the energy efficiency improvements in non-conventional food drying technologies. Trends Food Sci Technol. 2020;100:67–76. https://doi.org/10.1016/j.tifs.2020.03.014.
32. Amjad W, Raza MA, Asghar F, Munir A, Mahmood F, Husnain SN, Hussain MI, Kim JT. Advanced exergy analyses of a solar hybrid food dehydrator. Energies (Basel). 2022;15:1–15. https://doi.org/10.3390/en15041505.
33. Hossain MA, Amer BMA, Gottschalk K. Hybrid solar dryer for quality dried tomato. Dry Technol. 2008;26:1591–601. https://doi.org/10.1080/07373930802467466.
34. Mortezapour H, Ghobadian B, Minaei S, Khoshtaghaza MH. Saffron drying with a heat pump-assisted hybrid photovoltaic-thermal solar dryer. Dry Technol. 2012;30:560–6. https://doi.org/10.1080/07373937.2011.645261.
35. Lakshmi DVN, Muthukumar P, Layek A, Nayak PK. Drying kinetics and quality analysis of black turmeric (*Curcuma caesia*) drying in a mixed mode forced convection solar dryer integrated with thermal energy storage. Renew Energy. 2018;120:23–34. https://doi.org/10.1016/j.renene.2017.12.053.
36. Pal US, Khan MK, Mohanty SN. Heat pump drying of green sweet pepper. Dry Technol. 2008;26:1584–90. https://doi.org/10.1080/07373930802467144.
37. Chapchaimoh K, Poomsa-Ad N, Wiset L, Morris J. Thermal characteristics of heat pump dryer for ginger drying. Appl Therm Eng. 2016;95:491–8. https://doi.org/10.1016/j.applthermaleng.2015.09.025.
38. Şevik S, Aktaş M, Doğan H, Koçak S. Mushroom drying with solar assisted heat pump system. Energy Convers Manag. 2013;72:171–8. https://doi.org/10.1016/j.enconman.2012.09.035.

Publisher's Note Springer Nature remains neutral with regard to jurisdictional claims in published maps and institutional affiliations.